Monthly Notices
of the
ROYAL ASTRONOMICAL SOCIETY

MNRASL **444,** L63–L67 (2014) doi:10.1093/mnrasl/slu117

The rarity of star formation in brightest cluster galaxies as measured by *WISE*

Amelia Fraser-McKelvie,[1,2]★ Michael J. I. Brown[1,2] and Kevin A. Pimbblet[1,2,3]

[1]*School of Physics, Monash University, Clayton, VIC 3800, Australia*
[2]*Monash Centre for Astrophysics (MoCA), Monash University, Clayton, VIC 3800, Australia*
[3]*Department of Physics and Mathematics, University of Hull, Cottingham Road, Kingston-upon-Hull HU6 7RX, UK*

Accepted 2014 July 18. Received 2014 July 16; in original form 2014 May 12

ABSTRACT

We present the mid-infrared star formation rates of 245 X-ray selected, nearby ($z < 0.1$) brightest cluster galaxies (BCGs). A homogeneous and volume limited sample of BCGs was created by X-ray selecting clusters with $L_x > 1 \times 10^{44}$ erg s^{-1}. The *Wide-Field Infrared Survey Explorer* (*WISE*) All WISE Data Release provides the first measurement of the 12 μm star formation indicator for all BCGs in the nearby Universe. Perseus A and Cygnus A are the only galaxies in our sample to have star formation rates of $> 40\,M_\odot\,yr^{-1}$, indicating that these two galaxies are highly unusual at current times. Stellar populations of 99 ± 0.6 per cent of local BCGs are (approximately) passively evolving, with star formation rates of $<10\,M_\odot\,yr^{-1}$. We find that in general, star formation produces only modest BCG growth at the current epoch.

Key words: galaxies: clusters: general – galaxies: elliptical and lenticular, cD – galaxies: star formation – infrared: galaxies.

1 INTRODUCTION

Brightest cluster galaxies (BCGs) are massive, highly luminous ellipticals located at the bottom of a galaxy cluster's potential well. They differ from other large elliptical galaxies in size and velocity dispersion (e.g. von der Linden et al. 2007) and are often offset from the cluster red sequence (Bernardi et al. 2007; Bildfell et al. 2008), indicating differences in stellar populations and assembly histories (e.g. Brough et al. 2007; Liu et al. 2008). In the local Universe, the bulk of BCGs are red, early-type galaxies with spectra lacking emission lines. Any activity is largely quenched, likely due to a combination of dwindling merger activity and successful feedback mechanisms such as virial shock heating and active galactic nucleus (AGN) feedback (e.g. Binney & Tabor 1995; Voit & Donahue 2005; Dekel & Birnboim 2006; De Lucia & Blaizot 2007, and references therein).

Despite the predominantly quiescent population at current times, many BCGs possess trickles of star formation (e.g. Bildfell et al. 2008; Pipino et al. 2009; Ford & Bregman 2013). The central cluster environment is known to affect BCG star formation rates (SFRs), for example, the presence of a cooling flow is likely to trigger star formation (e.g. O'Dea et al. 2008; Stott et al. 2008; Donahue 2009; Hicks, Mushotzky & Donahue 2010; Rawle et al. 2012, and references therein).

Cooling flow clusters, or clusters with low central gas entropy, were found to produce infrared (IR) and ultraviolet (UV) excess in the X-ray selected cluster sample of Hoffer et al. (2012). Of the 243 BCGs in the Hoffer et al. (2012) sample, BCGs located in low central gas entropy clusters had an excess above that expected for purely old stellar emission of 43 and 38 per cent in the IR and UV, respectively. SFRs determined from the excess emission were moderate, and of all galaxies in the local Universe (defined as $z < 0.1$), only Perseus A and Cygnus A possessed SFRs $>10\,M_\odot\,yr^{-1}$ (34 and 95 $M_\odot\,yr^{-1}$, respectively). The Hoffer et al. (2012) sample was heterogeneous but uniformly characterized, including only clusters that had been observed by *Chandra*.

Optically derived BCG SFRs were provided for the X-ray selected sample of Crawford et al. (1999). Emission line spectra comprised 27 per cent of the BCG sample, and a further 6 per cent had only N II in emission and Hα in absorption. After fitting a stellar spectra template to the galaxies in their sample with high Hα luminosities, they found optically derived SFRs of < 1–10 s of $M_\odot\,yr^{-1}$. One cluster at a higher redshift (Abell 1835, $z = 0.253$) had a BCG with an SFR of 125 $M_\odot\,yr^{-1}$.

At $z > 1$, cluster samples with star-forming central galaxies are common (e.g. Brodwin et al. 2013). At intermediate redshifts there are some examples of starburst BCGs, such as the Phoenix cluster ($z = 0.596$) BCG which has an SFR of $740\,M_\odot\,yr^{-1}$

★ E-mail: amelia.mckelvie@monash.edu

(McDonald et al. 2012). In the local Universe, examples of star-forming BCGs are rare, but Perseus A (NGC 1275) is an exception to the typically quiescent BCG population. Displaying optical emission lines (e.g. Fabian et al. 2008), a type 1 Seyfert nucleus (e.g. Burbidge & Burbidge 1965) and cold molecular gas near the core (e.g. Fabian et al. 1994; Bridges & Irwin 1998; Edge & Frayer 2003), Perseus A possesses a high SFR (Wirth, Kenyon & Hunter 1983), despite significant AGN activity (as demonstrated by Fabian et al. 2008). In fact, Perseus A is the archetypal example of AGN feedback in the local Universe, despite its high SFR.

Whether the activity of Perseus A is unique or a common stage in a BCG's life cycle is unknown. While it is clear that star-forming BCGs do exist, and that a significant population of them can be found in environments where we would expect star formation to occur (e.g. cool-core clusters), the actual fraction of *all* low redshift BCGs that possess star formation is unknown, as is the significance of the star formation. Is it great enough to add an appreciable amount to the overall mass of the galaxy? Is Perseus A unique in its high star formation, or is it just a phase all BCGs pass through? To examine these questions, a complete, local sample of BCGs is required.

This Letter quantifies the fraction of star-forming BCGs by creating an X-ray luminosity limited catalogue of local BCGs (Section 2), measuring the IR photometry using the recently released All WISE survey in Section 3, and using the 12 μm band to estimate the SFRs and specific star formation rates (sSFR) in Section 4. The cosmology used throughout this Letter is $H_0 = 70\,\mathrm{km\,s^{-1}\,Mpc^{-1}}$, $h_0 = H_0/100$, $\Omega_\mathrm{M} = 0.3$ and $\Omega_\Lambda = 0.7$. All magnitudes are in the Vega system.

2 BCG SAMPLE

A homogeneous BCG sample was created based on X-ray selection of host clusters with $L_x > 1 \times 10^{44}\mathrm{erg\ s^{-1}}$ in the *ROSAT* 0.1–2.4 keV band, corresponding to an approximate cluster mass of $M_{2500} \gtrsim 1 \times 10^{14}\,\mathrm{M_\odot}$ (Hoekstra et al. 2011). Selecting only X-ray luminous clusters ensures BCGs are located in comparably massive clusters. X-ray clusters were taken from the *ROSAT* Brightest Cluster Survey (BCS; Ebeling et al. 1998), extended BCS (Ebeling et al. 2000), the X-ray Brightest Abell Clusters Survey (Ebeling et al. 1996), the *ROSAT* North Ecliptic Pole Survey (e.g. Gioia et al. 2001), the *ROSAT*-ESO flux limited X-ray galaxy cluster survey (e.g. Böhringer et al. 2001) and The Northern *ROSAT* All-Sky Galaxy Cluster Survey (Böhringer et al. 2000), and queried using the Base de Données Amas de Galaxies (BAX; Sadat et al. 2004). The redshift of the sample was limited to $z < 0.1$, creating a sample of 267 nearby, X-ray bright clusters where the completeness limit of each of the input surveys was at least 80 per cent. As we wished to identify BCGs regardless of their SFR, no colour selection criteria were applied.

We identified 144 BCGs by cross-matching the cluster sample with the BCG catalogues of Stott et al. (2008), Coziol et al. (2009) and Wen, Han & Liu (2012). The remaining 123 unmatched clusters were inspected visually by AFM and KAP in both optical (Digitized Sky Survey) and IR (Two Micron All Sky Survey, 2MASS) images, along with a NASA/IPAC Extragalactic Database object search to verify the redshifts of the candidate BCGs. The vast majority of identifications were unambiguous, and in all cases, the brightest galaxy in the 2MASS *K*-band at the cluster redshift was chosen as the BCG.

In some cases, clusters had to be eliminated from the sample if it was not clear which galaxy was the BCG. Reasons for this included mergers of galaxies of similar magnitude (e.g. Abell 3825), source confusion (e.g. Abell 523), or unavailable redshift information for any candidate BCG (e.g. Abell 72). Clusters were also eliminated from the sample if the *Wide-Field Infrared Survey Explorer* (*WISE*) image showed source contamination from nearby saturated stars, or in six cases, the same cluster was entered twice into BAX under different names.

The final sample comprises 245 BCGs, covering both the Northern and Southern hemispheres, for which source photometry was extracted for from the All WISE Data Release Catalog.

3 PHOTOMETRY

WISE (Wright et al. 2010) completed a whole-sky survey in four IR bands: 3.4, 4.6, 12 and 22 μm (denoted bands W1–W4). Bands W1 and W2 coincide with the Rayleigh–Jeans tail of the stellar emission of a galaxy and provide an accurate estimate of stellar mass. The W3 band is sensitive to warm dust and polycyclic aromatic hydrocarbon emission associated with H II regions and molecular clouds.

Photometry for each BCG in the sample was extracted in all bands from the newly released All WISE Source Catalog, combining improved multi-epoch photometry from the *WISE* and NeoWISE surveys. We use the recommended approach for extended sources from the All WISE explanatory statement, (Cutri et al. 2013) briefly described below.

Sources that are resolved and associated with a 2MASS Extended Source Catalog (XSC) object (232 galaxies in our sample) are measured with elliptical apertures made using apertures scaled from 2MASS XSC apertures to account for the *WISE* PSF. All WISE sources that are associated with a 2MASS XSC object but are not resolved in *WISE* (7 galaxies) are modelled with profile fit photometry to avoid overestimating flux. For the four sources that are extended but not associated with a 2MASS XSC object, a fixed aperture size of 16.5 arcsec based on curve of growth was used with the prescribed aperture correction applied to each band. Where the signal-to-noise ratio is less than 2 in the W3 band, the magnitude of the 95 per cent confidence brightness upper limit is instead used for analysis.

4 STAR FORMATION RATES AND BCG GROWTH

To illustrate the IR excess of BCGs, in Fig. 1, we plot the *WISE* colours of BCGs with W3 band detections. Like local ellipticals (Jarrett et al. 2011), the locus of the BCG sample is slightly offset from the origin at around W2−W3 ∼ 0.4 (corresponding to an approximately Rayleigh–Jeans spectrum), with seven outlying BCGs residing in the star-forming region of the plot. The 1σ photometric scatter is ∼0.3 mag, and we expect 45 galaxies redder than this threshold, more than the amount of blue galaxies, showing this colour distribution is not the result of photometric scatter. Just 3 ± 1 per cent of the sample have an IR excess measured by a W2−W3 colour greater than 1.5, corresponding to systems likely dominated by star formation (Cluver et al. 2014).

A Hα-derived SFR relation was determined for the *WISE* W3 band by Cluver et al. (2014) by cross-matching *WISE* sources with those with available SFRs from GAMA I (Gunawardhana et al. 2013):

$$\log\ \mathrm{SFR_{H\alpha}(M_\odot\ yr^{-1})} = 1.13 \log \nu L_\mathrm{W3}(\mathrm{L_\odot}) - 10.24. \quad (1)$$

We subtract stellar emission using the Cohen et al. (1992) stellar calibration model fitted to the W2 band, which closely resembles

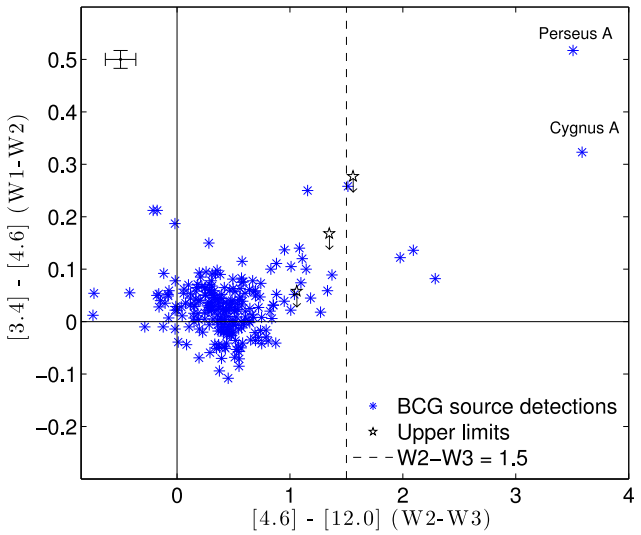

Figure 1. *WISE* colour–colour diagram for BCGs in the sample, and representative error bars in the top-left corner. Galaxies with [4.6]–[12.0]>1.5 have an excess of IR emission in the W3 band, and are most likely to be dominated by star formation (Cluver et al. 2014). The bulk of the sample lie offset from the zero-point by ∼0.4 mag, indicating they are redder than the typical Rayleigh–Jeans region, in line with Jarrett et al. (2011). Two of the galaxies in the BCG sample are not detected in the W3 band, or did not have corresponding elliptical magnitudes in the case of the extended sources, so are not included here.

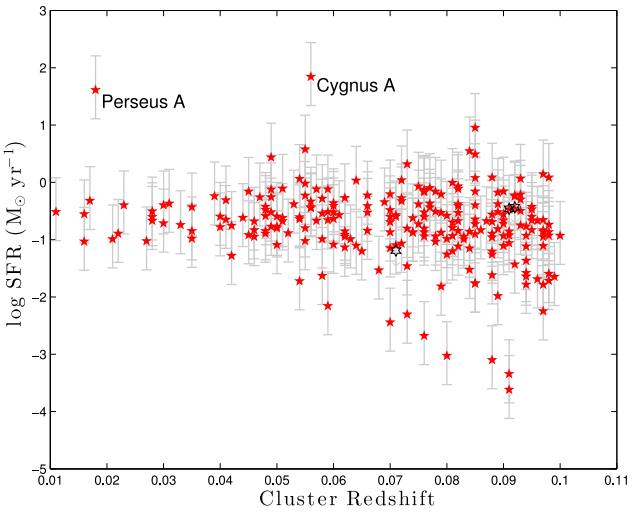

Figure 2. BCG sample SFRs as calculated by the relation in Cluver et al. (2014) as a function of cluster redshift with uncertainties derived from the scatter in equation (1) (Cluver, private communication). Stellar emission has been subtracted from the W3 measurements to leave predominantly emission from hot dust. The unfilled markers with arrows represent upper limits. SFRs are less than $10\,M_\odot\ yr^{-1}$ for 99 ± 0.6 per cent of the sample, with the main exceptions of Perseus A and Cygnus A, exhibiting high SFRs in comparison to the rest of the sample.

the tail of the Rayleigh–Jeans spectrum. Subtracting this primarily stellar emission from the W3 band leaves emission solely from warm dust. Hence L_{W3} is the stellar emission-subtracted IR luminosity in the *WISE* W3 band, and ν the effective frequency of the W3 passband.

We modelled the *WISE* apparent and absolute magnitudes of galaxies as a function of both redshift and observed colour using the spectral energy distribution (SED) templates of Brown et al. (2014). The *k*-corrections as a function of colour at a given redshift were estimated and applied. *k*-corrections are −0.3 magnitudes or less for the bulk of the galaxies in our sample, corresponding to a $\Delta SFR \sim 0.04\,M_\odot\ yr^{-1}$.

The SFRs as calculated by equation (1) are plotted against cluster redshift in Fig. 2. Of the BCG sample with detections in the W3 band, 99 ± 0.6 per cent have SFRs of $10\,M_\odot\ yr^{-1}$ or less. Two significant outliers, Perseus A and Cygnus A, have SFRs of 41 and $70\,M_\odot\ yr^{-1}$, respectively. BCG photometry, along with stellar mass and SFR estimates are listed in Table 1. The dominant uncertainty is that from the scatter from the relation of equation (1) (Cluver, private communication).

We matched our BCG sample to the total IR and UV-derived SFRs of Hoffer et al. (2012), and the optically derived SFRs of Crawford et al. (1999), with 18, 49 and 6 matches to our sample, respectively. For SFRs $>10\,M_\odot\ yr^{-1}$, our measured SFRs agree with Hoffer et al. (2012) IR SFR within 26 per cent. IR SED fits are available for Perseus A and Cygnus A (e.g. Mittal et al. 2012; Privon et al. 2012), providing SFRs of 24 ± 1 and $\sim 10\,M_\odot\ yr^{-1}$, respectively. These SFRs are lower than those derived for this study (41 and $70\ M_\odot\ yr^{-1}$ for Perseus A and Cygnus A, respectively), and for the Hoffer et al. (2012) total IR and UV derived SFRs.

There is considerable scatter between different SFR estimates for BCGs with SFRs $<10\,M_\odot\ yr^{-1}$, and the Cluver et al. (2014) relation may underestimate SFRs for low IR luminosity galaxies. In the low redshift ($z < 0.05$) regime, the Cluver et al. (2014) relation works well for galaxies with SFRs $> 3M_\odot\ yr^{-1}$, but may underestimate SFRs lower than this. Despite this, for SFRs $<3M_\odot\ yr^{-1}$, our SFRs agree with the multiwavelength-derived SFRs of Hoffer et al. (2012) and Crawford et al. (1999) within 1 dex. Importantly, the scatter introduced in the low SFR sample either by the SFR relation, or possible excess emission by AGN contamination (e.g. Donley et al. 2008; Donoso et al. 2012) is not enough to push any low SFR galaxies into the highly star-forming regime, preserving our primary conclusion that only a tiny fraction ($<1 \pm 0.6$ per cent) of local Universe BCGs are highly star forming.

BCG stellar masses were determined using the relation of Wen et al. (2013) from the *WISE* W1 band:

$$\log\left(\frac{M_*}{M_\odot}\right) = (-0.040 \pm 0.001) + (1.120 \pm 0.001)\log \nu L_{W1}(L_\odot), \quad (2)$$

where L_{W1} is the W1 band luminosity. Fig. 3 shows the sSFRs of the entire sample as a function of cluster X-ray luminosity. Most BCGs show low sSFR, of the order of $10^{-12}\ yr^{-1}$. Again, Perseus A and Cygnus A stand out with sSFR of almost $10^{-10}\ yr^{-1}$, and while these SFRs will double the stellar mass of the galaxies over a Hubble time, they are unlikely to be sustained, as both systems are likely to be undergoing merger-induced star formation (e.g. Holtzman et al. 1992; Markevitch, Sarazin & Vikhlinin 1999; Conselice, Gallagher & Wyse 2001, and references therein). Both Perseus A and Cygnus A are located in highly X-ray luminous clusters, suggesting there may be a slight preference for high L_X clusters to host highly star-forming BCGs (e.g. O'Dea et al. 2008). Perseus A and Cygnus A are also both located in cool core clusters (e.g. Hoffer et al. 2012).

Thus, we conclude that while some star formation is occurring, this constitutes only modest BCG growth at current times.

Table 1. *WISE* photometry and derived SFRs of BCGs in the BAX X-ray selected cluster sample with $L_x > 1 \times 10^{44}\,\mathrm{erg\,s^{-1}}$. When there was no W3 detection for a BCG, the photometry and SFRs are left blank. Similarly, for when the BCG could not be unambiguously identified, we report the cluster coordinates and leave the stellar mass and SFRs blank. Reasons for each BCG exclusion are listed in the footnotes. Table 1 is published in its entirety in the electronic edition.

Cluster name	BCG RA (°, J2000)	BCG Dec. (°, J2000)	Cluster z	Cluster $L_x(10^{44}$ erg s^{-1})	W1 (mag)	W2 (mag)	W3 (mag)	Stellar mass ($10^{10}\,M_\odot$)	SFR ($M_\odot\,yr^{-1}$)
RXC J0003.8+0203	0.9570	2.0665	0.092	1.50	11.51 ± 0.01	11.47 ± 0.01	11.07 ± 0.21	$64.5^{+1.13}_{-1.11}$	$0.35^{+0.41}_{-0.09}$
RXC J0011.3−2851	2.8403	−28.8547	0.062	2.42	11.23 ± 0.01	11.21 ± 0.01	11.03 ± 0.16	$34.1^{+0.62}_{-0.61}$	$0.07^{+0.09}_{-0.02}$
RXC J0013.6−1930	3.3917	−19.4838	0.094	2.26	12.19 ± 0.01	12.10 ± 0.01	11.84 ± 0.28	$33.5^{+0.58}_{-0.57}$	$0.12^{+0.14}_{-0.03}$
RXC J0017.5−3511	4.3958	−35.1833	0.095	1.22	12.54 ± 0.01	12.49 ± 0.02	11.89 ± 0.20	$24.0^{+0.40}_{-0.39}$	$0.22^{+0.26}_{-0.06}$
ABELL 0021[a]	5.1545	28.6590	0.095	2.64	–	–	–	–	–
IVZW 015	5.4033	28.0505	0.094	1.72	11.95 ± 0.01	11.89 ± 0.01	12.06 ± 0.36	$43.3^{+0.75}_{-0.73}$	$0.02^{+0.03}_{-0.01}$
RXC J0034.2−0204	8.5612	−2.0846	0.082	2.40	11.37 ± 0.01	11.34 ± 0.01	10.49 ± 0.10	$56.7^{+1.01}_{-0.99}$	$0.86^{+1.02}_{-0.22}$
RXC J0034.6−0208[b]	8.6500	−2.1400	–	–	–	–	–	–	–
ABELL 0072[b]	9.6366	45.7247	–	–	–	–	–	–	–
ABELL 0077	10.1180	29.5557	0.071	1.74	11.28 ± 0.01	11.26 ± 0.01	10.83 ± 0.13	$44.5^{+0.49}_{-0.48}$	$0.25^{+0.13}_{-0.03}$

Note: [a]No extended source data in All WISE catalogue. [b]Source confusion.

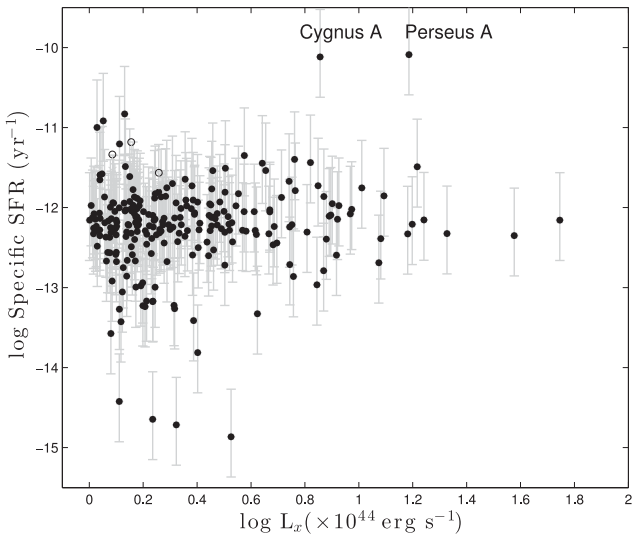

Figure 3. sSFRs of BCGs in the sample as a function of cluster X-ray luminosity. The unfilled circles with arrows represent upper limits. There is little trend in sSFR with increasing L_x, and with the exception of Perseus A and Cygnus A, all BCGs at $z < 0.1$ have sSFRs of less than 1 per cent per Gyr.

5 SUMMARY

We employed new mid-IR photometry from All WISE to measure the SFRs of 245 BCGs in X-ray selected clusters at $z < 0.1$. Our BCG catalogue was created by selecting X-ray bright clusters with $L_x > 1 \times 10^{44}\,\mathrm{erg\,s^{-1}}$ in the *ROSAT* 0.1–2.4 keV band.

For the first time, 12 μm photometry (an SFR indicator) was measured for a large sample of local BCGs, and we find that the majority have IR SEDs that differ from simple Rayleigh–Jeans spectra. The bulk of BCGs at $z < 0.1$ possess little or no star formation at current times, with inferred SFRs of less than $10\,M_\odot\,yr^{-1}$ for 99 ± 0.6 per cent of local BCGs. While the SFRs of BCGs with very low IR luminosities may have been underestimated, this does not impact our primary conclusion that only a tiny fraction of BCGs possess SFRs $> 10\,M_\odot\,yr^{-1}$. Hence, we determine that only modest BCG growth is occurring as a result of star formation at the current epoch.

Perseus A and Cygnus A are the BCGs with the highest SFRs in the $z < 0.1$ Universe (41 and $70\,M_\odot\,yr^{-1}$, respectively), calculated from hot dust emission. Whilst Perseus A is the archetypal example of AGN feedback, it is an exceptional BCG within the local Universe.

ACKNOWLEDGEMENTS

The authors wish to thank the referee for thoughtful and insightful comments that have improved this manuscript, and Alain Blanchard, Michelle Cluver and Tom Jarrett for helpful conversations on the topic. AFM acknowledges support from an Australian Postgraduate Award (APA), and a J. L. William postgraduate award. MJIB acknowledges financial support from the Australian Research Council (DP110102174, FT100100280) and the Monash Research Accelerator Programme.

This research has made use of the X-Rays Clusters Database (BAX) which is operated by the Laboratoire d'Astrophysique de Tarbes-Toulouse (LATT), under contract with the Centre National d'Etudes Spatiales (CNES).

This publication makes use of data products from the Two Micron All Sky Survey, which is a joint project of the University of Massachusetts and the Infrared Processing and Analysis Center/California Institute of Technology, funded by the National Aeronautics and Space Administration and the National Science Foundation.

All WISE makes use of data from *WISE*, which is a joint project of the University of California, Los Angeles, and the Jet Propulsion Laboratory/California Institute of Technology, and NEOWISE, which is a project of the Jet Propulsion Laboratory/California Institute of Technology. *WISE* and NEOWISE are funded by the National Aeronautics and Space Administration.

This research has made use of the NASA/IPAC Extragalactic Database (NED), which is operated by the Jet Propulsion Laboratory, California Institute of Technology, under contract with the National Aeronautics and Space Administration.

REFERENCES

Bernardi M., Hyde J. B., Sheth R. K., Miller C. J., Nichol R. C., 2007, AJ, 133, 1741
Bildfell C., Hoekstra H., Babul A., Mahdavi A., 2008, MNRAS, 389, 1637
Binney J., Tabor G., 1995, MNRAS, 276, 663
Böhringer H. et al., 2000, ApJS, 129, 435
Böhringer H. et al., 2001, A&A, 369, 826
Bridges T. J., Irwin J. A., 1998, MNRAS, 300, 967
Brodwin M. et al., 2013, ApJ, 779, 138
Brough S., Proctor R., Forbes D. A., Couch W. J., Collins C. A., Burke D. J., Mann R. G., 2007, MNRAS, 378, 1507
Brown M. J. I. et al., 2014, ApJS, 212, 18
Burbidge E. M., Burbidge G. R., 1965, ApJ, 142, 1351
Cluver M. E. et al., 2014, ApJ, 782, 90
Cohen M., Walker R. G., Barlow M. J., Deacon J. R., 1992, AJ, 104, 1650
Conselice C. J., Gallagher J. S., III, Wyse R. F. G., 2001, AJ, 122, 2281
Coziol R., Andernach H., Caretta C. A., Alamo-Martínez K. A., Tago E., 2009, AJ, 137, 4795
Crawford C. S., Allen S. W., Ebeling H., Edge A. C., Fabian A. C., 1999, MNRAS, 306, 857
Cutri R. M. et al., 2013, Explanatory Supplement to the AllWISE Data Release Products, available at: http://adsabs.harvard.edu/abs/2013wise.rept....1C
De Lucia G., Blaizot J., 2007, MNRAS, 375, 2
Dekel A., Birnboim Y., 2006, MNRAS, 368, 2
Donahue M., 2009, in Heinz S., Wilcots E., eds, AIP Conf. Ser. Vol. 1201, Signatures of Star Formation in Brightest Cluster Galaxies. Am. Inst. Phys., New York, p. 177
Donley J. L., Rieke G. H., Pérez-González P. G., Barro G., 2008, ApJ, 687, 111
Donoso E. et al., 2012, ApJ, 748, 80
Ebeling H., Voges W., Bohringer H., Edge A. C., Huchra J. P., Briel U. G., 1996, MNRAS, 281, 799
Ebeling H., Edge A. C., Bohringer H., Allen S. W., Crawford C. S., Fabian A. C., Voges W., Huchra J. P., 1998, MNRAS, 301, 881
Ebeling H., Edge A. C., Allen S. W., Crawford C. S., Fabian A. C., Huchra J. P., 2000, MNRAS, 318, 333
Edge A. C., Frayer D. T., 2003, ApJ, 594, L13
Fabian A. C., Arnaud K. A., Bautz M. W., Tawara Y., 1994, ApJ, 436, L63
Fabian A. C., Johnstone R. M., Sanders J. S., Conselice C. J., Crawford C. S., Gallagher J. S., III, Zweibel E., 2008, Nature, 454, 968
Ford H. A., Bregman J. N., 2013, ApJ, 770, 137
Gioia I. M., Henry J. P., Mullis C. R., Voges W., Briel U. G., Böhringer H., Huchra J. P., 2001, ApJ, 553, L105
Gunawardhana M. L. P. et al., 2013, MNRAS, 433, 2764
Hicks A. K., Mushotzky R., Donahue M., 2010, ApJ, 719, 1844
Hoekstra H., Donahue M., Conselice C. J., McNamara B. R., Voit G. M., 2011, ApJ, 726, 48
Hoffer A. S., Donahue M., Hicks A., Barthelemy R. S., 2012, ApJS, 199, 23
Holtzman J. A. et al., 1992, AJ, 103, 691
Jarrett T. H. et al., 2011, ApJ, 735, 112
Liu F. S., Xia X. Y., Mao S., Wu H., Deng Z. G., 2008, MNRAS, 385, 23
McDonald M. et al., 2012, Nature, 488, 349
Markevitch M., Sarazin C. L., Vikhlinin A., 1999, ApJ, 521, 526
Mittal R. et al., 2012, MNRAS, 426, 2957
O'Dea C. P. et al., 2008, ApJ, 681, 1035
Pipino A., Kaviraj S., Bildfell C., Babul A., Hoekstra H., Silk J., 2009, MNRAS, 395, 462
Privon G. C., Baum S. A., O'Dea C. P., Gallimore J., Noel-Storr J., Axon D. J., Robinson A., 2012, ApJ, 747, 46
Rawle T. D. et al., 2012, ApJ, 747, 29
Sadat R., Blanchard A., Kneib J.-P., Mathez G., Madore B., Mazzarella J. M., 2004, A&A, 424, 1097
Stott J. P., Edge A. C., Smith G. P., Swinbank A. M., Ebeling H., 2008, MNRAS, 384, 1502
Voit G. M., Donahue M., 2005, ApJ, 634, 955
von der Linden A., Best P. N., Kauffmann G., White S. D. M., 2007, MNRAS, 379, 867
Wen Z. L., Han J. L., Liu F. S., 2012, ApJS, 199, 34
Wen X.-Q., Wu H., Zhu Y.-N., Lam M. I., Wu C.-J., Wicker J., Zhao Y.-H., 2013, MNRAS, 433, 2946
Wirth A., Kenyon S. J., Hunter D. A., 1983, ApJ, 269, 102
Wright E. L. et al., 2010, AJ, 140, 1868

SUPPORTING INFORMATION

Additional Supporting Information may be found in the online version of this article:

Table 1. *WISE* photometry and derived SFRs of BCGs in the BAX X-ray selected cluster sample with $L_x > 1 \times 10^{44}$ erg s^{-1} (http://mnras.oxfordjournals.org/lookup/suppl/doi:10.1093/mnrasl/slu117/-/DC1).

Please note: Oxford University Press is not responsible for the content or functionality of any supporting materials supplied by the authors. Any queries (other than missing material) should be directed to the corresponding author for the Letter.

This paper has been typeset from a TEX/LATEX file prepared by the author.